Research on the Related Properties of EVM/$Al(OH)_3$/SiO_2 Composites Applied for Halogen-Free Flame Retardant Cable Insulation and Jacket

Lichun Wang,[1,2] Genlin Wang,[1,2] Pingkai Jiang[1,2]

[1]*Department of Polymer Science and Engineering Polymer, School of Chemistry and Chemical Engineering, Shanghai Jiao Tong University, Shanghai 200240, People's Republic of China*
[2]*Department of Polymer Science andEngineering Polymer, Shanghai Key Lab of Electric Insulation and Thermal Aging, Shanghai Jiao TongUniversity, Shanghai 200240, People's Republic of China*

Received 25 October 2009; accepted 4 August 2010
DOI 10.1002/app.33149
Published online 13 October 2010 in Wiley Online Library (wileyonlinelibrary.com).

ABSTRACT: The halogen-free flame retardant (HFFR) ethylene-vinyl acetate copolymer (EVM)/ATH/SiO_2 composites have been prepared by melting compounding method, and the flame retardant, thermal stability, rheological, electrical, and mechanical properties have been investigated by cone calorimeter, LOI, UL-94, TG, FE-SEM, rotational rheometer, dielectric breakdown, and ultimate tensile. The results indicate that the flame retardant of EVM vulcanizates is improved and the fire jeopardizing is dramatically reduced due to the addition of ATH. It is necessary that sufficient loading of ATH ($\geq$120 phr) is needed to reach essential level (LOI $>$ 30; V-0 rating) of flame retardant for HFFR EVM/ATH/SiO_2 composites used as cable in industry. The rheological characteristics show that at all the measurement frequencies, the storage and loss modulus of the composites increase monotonously as the concentration of ATH filler increases, while the complex viscosity and tan delta present reverse trend. And also, it has been found that the HFFR composites at high filler concentrations still keep good mechanical and electrical properties, which is very important for practical applications as cable. © 2010 Wiley Periodicals, Inc. J Appl Polym Sci 120: 368–378, 2011

Key words: ethylene-vinyl acetate copolymer; aluminum hydroxide; composites; halogen-free flame retardant; cable; rheology

INTRODUCTION

The susceptibility of polymeric materials to fire continues to be of great concern all over the world. Cable materials are of no exception. The stringent conditions set by statutory governmental regulations for the use of flame retardants (FRs) demand development of newer and better FRs. Although brominated FRs are the effective FRs on the market, there has been, in recent years, much concern worldwide over their use because they give rise to toxic gases and smoke.[1–8] Facing the disastrous loss and casualty by fire, more and more researchers think that the application of HFFR materials with low emission of smoke and toxicity is necessary. Many investigations have demonstrated that inorganic hydroxide fillers, such as magnesium hydroxide (MDH) and aluminum hydroxide (ATH), are excellent nontoxic and smoke-suppressing HFFR additives.[9–12] They are commonly used in polyolefins for manufacturing HFFR and low smoke cables. These compounds act in both the condensed phase and the gas phase. Their thermal decomposition follows an endothermic reaction to decrease the temperature of materials and releases water into the gas phase to dilute the flame.[13] However, as a hydrophilic inorganic filler, it is difficult to disperse evenly in the hydrophobic polymer matrix. In addition, low effectiveness makes it necessary to incorporate at a very high content in polymers to gain a satisfying low flammability. Both poor dispersion and high loadings deteriorate the material's mechanical properties, especially toughness.[14] Although there has been many studies focusing mainly on this problem, and it is a pity that no perfect project has been found. Wei et al.[15] has reported that the synergistic flame retardant effect of SiO_2 can be found in low density polyethylene/ethylene vinyl acetate/ATH blends; Jiao and Chen[16] found that synergistic flame Retardant effect of cerium oxide in ethylene-vinyl acetate/aluminum hydroxide blends can be obtained.

Ethylene-vinyl acetate copolymer is highly elastomeric, and tolerates high filler loadings while retaining its flexible properties, so it is widely used in combination with metal hydroxide FRs as zero-halogen specification electric cable and packaging materials.[17–20] As the vinyl acetate content increases, the

Correspondence to: P. Jiang (pkjiang@sjtu.edu.cn).

TABLE I
Formulations of HFFR EVM/ATH/SiO_2 Composites Used as Cable

Code	EVM	ATH (phr)	SiO_2 (phr)	DCP (phr)	TAIC (phr)	DDA (phr)	$ZnSt_2$ (phr)
EVM-1	100	0	5	2.0	0.5	0.5	0.5
EVM-2	100	60	5	2.0	0.5	0.5	0.5
EVM-3	100	120	5	2.0	0.5	0.5	0.5
EVM-4	100	160	5	2.0	0.5	0.5	0.5
EVM-5	100	200	5	2.0	0.5	0.5	0.5

copolymer presents increasing polarity but lower crystallization, and therefore different mechanical behavior.[21] Bhattacharya has reported that increasing the vinyl acetate content was necessary to achieve greater clay-polymer interaction and higher intercalation of clay platelets for resin-clay nanocomposites. The increasing polarity with increasing vinyl acetate content is apparently useful in imparting a high degree of polymer-filler surface interaction, which is very important for polymer composites with high loading fillings in practical applications. Ethylene-vinyl acetate copolymer rubber (EVM), as a copolymer of ethylene and high content of vinyl acetate (generally, the vinyl acetate content is 40–80%), is suitable for using as HFFR wire and cable insulating or sheathing materials because of its good compatibility with inorganic FRs, good resistance to oil, good heat-resistant and good flame-retardant properties.[22–24] Qu and Li[22] has reported that the effects of gamma irradiation on the properties of flame-retardant EVM/magnesium hydroxide blends and indicates that over 60 wt% MDH loading is required to obtain an adequate level of flame retardancy for poly(ethylene-*co*-acetate)/MDH blends.

In this study, it is mainly devoted to investigating the effects of HFFR additive ATH on the flame retardant, electrical, rheological, and mechanical properties of EVM/ATH/SiO_2 composites crosslinked by dicumyl peroxide (DCP). Through the measurements of cone calorimeter, limiting oxygen index (LOI), UL-94, thermogravimetric analysis (TGA), gel content, ultimate tensile, dielectric, and rheological properties, the aim in the present work is mainly to develop HFFR composites that can be used in wire and cable industry.

EXPERIMENTAL

Materials

A commercial cable grade EVM rubber (Levaprene 500HV) was kindly supplied by Bayer Co., Germany. The vinyl acetate content was 50 wt %, the Mooney viscosity was ML_{1+4} (100°C) = 27 ± 4, the MFI (g/10 min) ≤ 5, and the density was 1.00 g/cm^3.

Aluminum hydroxide (ATH) supplied by Nabaltec GmbH, modified by vinylmethyldimethoxy silane, with an average particle size of 1.0 μm, the specific surface area of 6.0 m^2/g, was used as a flame retardant filler.

The nano-silicon dioxide (SiO_2) with an average particle size of 20 nm, the specific surface area of 400 m^2/g, and coated by vinyltrimethoxy silane, was used as an intensifier produced by Nanjing HaiTai nano-material Co. Ltd, China.

DCP used as a crosslinking agent was 99.3% pure and obtained from Shanghai Gaoqiao Petroleum Co. Ltd, China.

Crosslinking coagent triallylisocyanurate (TAIC) and antioxidant dialkylated diphenylamine (DDA) were all supplied by Taizhou Huangyan Donghai chemical Co. Ltd, China.

Processing additive zinc stearate ($ZnSt_2$) was produced by China Medicine (Group) Shanghai Chemicals Reagent Corp. All the above materials were not further purified and used as received.

Preparation of samples and crosslinking

EVM chemically crosslinked cable formulations (Table I), containing different loading (0–200 phr, parts per hundred of resin) of inorganic additives (ATH) as flame retardant and quantitative loading of 5.0 phr SiO_2 as an intensifier, were prepared through the following several steps. First, all additives except DCP were mixed with resins for 8 min at 150°C with an internal mixer at a speed of 50 rpm. Then, the mixture was moved into a two-roll mill, and DCP was added at 110°C and mixed for 3–5 min. Finally, crosslinking of the mixtures were performed and samples of EVM vulcanizates were prepared by using the molding of sheets at 180°C for 10 min.

Measurement and characterization

Cone calorimeter test

Cone calorimeter uses a truncated conical heater element to irradiate test specimens at heat fluxes from 10 to 100 kW/m^2, thereby simulating a range of fire intensities. The technique is a small scale fire test, but it has been shown to provide data that correlate well with those from full-scale fire tests.[24] Cone calorimeter tests were carried out in duplicate, using a

35 kW/m^2 incident heat flux, following the procedures indicated in the ISO 5660 standard with a FTT cone calorimeter. Each specimen, of dimensions 100 × 100 × 3 mm^3, was wrapped in aluminum foil and placed on a mineral fiber blanket with the surface level with the holder, such that only the upper face was exposed to the radiant heater. The edge guard was used with all specimens, as was the recommended standard retaining grid to prevent excessive intumescence. The experimental error rate from the cone calorimeter test was about ± 5%. The cone calorimeter technique provides detailed information about ignition behavior, heat release, and smoke evolution during sustained combustion and some key parameters which are correlated well with real fire.[25]

Limiting oxygen index

The LOI value was measured using an HC-2 type instrument (Nanjing Analytical Instrument Factory, China) on the sheets of 120 × 6.5 × 3 mm^3 according to ASTM D 2863-77.

UL-94 test

The UL-94 vertical test was carried out using a CZF-1 type instrument (Nanjing Analytical Instrument Factory, China) on the sheets of 127 × 12.7 × 3 mm^3 according to ASTM D 635-77.

Thermogravimetric analysis (TGA)

The TGA data were obtained in air at a heating rate of 20°C/min by a Perkin–Elmer Q 50 thermogravimetric analyzer. In each case, a 5–10 mg sample was examined under the gas (air) flow rate of 5 × 10^{-5} m^3/min at the temperatures ranging from room temperature to 800°C.

Gel content

The gel content was determined by extracting the included EVM vulcanizate (m_1) which can be calculated from the formulations (Table I) for all samples in boiling xylene for 48 h. After being dried at 80°C, the remained EVM vulcanizate (m_2) was obtained through the inorganic additives were subtracted from the insoluble residue which was weighted. The average gel content was calculated as m_2/m_1. Five samples were analyzed to determine the average gel content for every given EVM vulcanizate sample.

Mechanical measurements

The tensile properties were measured on an Instron series IX 4465 material tester at a crosshead speed of 100 mm/min with dumbbell specimens (4 mm wide in the cross section) according to ASTM D 412-06a (Standard Test Methods for Vulcanized Rubber and Thermoplastic Elastomers-Tension). Meanwhile, the Shore A hardness was determined with a hand-held Shore A durometer according to ASTM D 2240-05 (Standard Test Method for Rubber Property - Durometer Hardness). All the tests were carried out at 25 ± 2°C.

Microstructure analyses by SEM

Scanning electron microscopic (SEM) analyses for the morphology of residues of combustion by cone calorimeter were made using a field emission scanning electron microscopy (FE-SEM, JEOL JEM-4701). The gold-coated samples to avoid accumulation of charges were analyzed at an accelerating voltage of 20 kV.

Dielectric property measurements

DC conductivity measurements were performed by using an EST-121 High Resistance Meter (Beijing EST Science and Technology Co., Ltd., China) according to ASTM D 257. Samples with thickness of around 1.0 mm were used for dielectric and current measurement.[26] Gold electrodes were evaporated on the front and rear surfaces of the samples (a front electrode, 50 mm in diameter, surrounded by a guard ring, and a back electrode deposited on the whole rear surface).

Dielectric breakdown testing was performed on an AHDZ-10/100 alternating current dielectric strength tester (Shanghai Lanpotronics Corp., Shanghai, China) according to ASTM D 149- 2004. The specimens were immersed in the pure silicon oil, between two 10-mm-diameter copper ball electrodes opposing to each other. The lower electrode was connected to earth and an increasing ac voltage was applied to the upper electrode with a rate of 2 KV/s until the sample failed. Five breakdown tests were performed on each specimen with thickness of around 1.0 mm, and the average dielectric breakdown strength was calculated.

Rheological measurement

A rotational rheometer, Gemini 200HR (Bohlin instruments, UK) with a parallel-plate geometry (diameter of 25 mm), was used for rheological measurements. Small amplitude oscillatory shear was performed in the frequency range 0.1–100 rad/s at 110°C. A strain of less than 5% was used, which was in the linear viscoelastic regime for all samples. All the samples were tested before crosslinking.

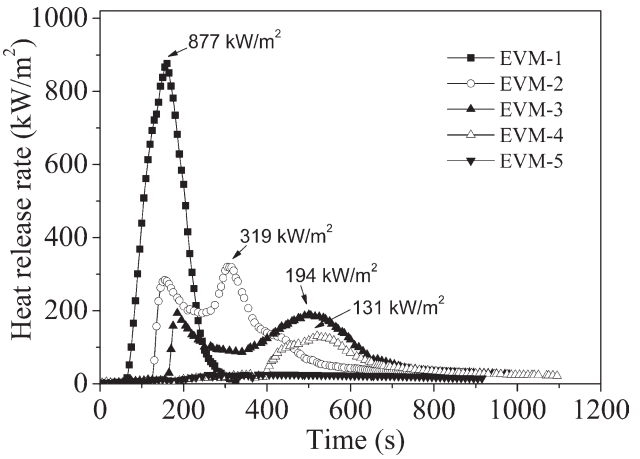

Figure 1 HRRs versus burning time for EVM/ATH/SiO_2 composites filled with different loading of ATH

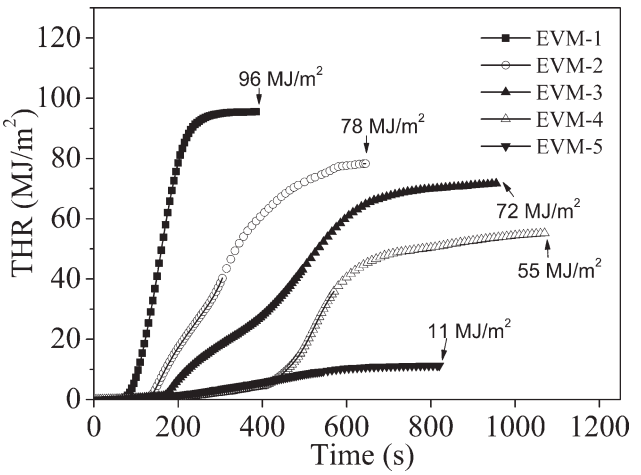

Figure 2 THRs versus burning time for EVM/ATH/SiO_2 composites filled with different loading of ATH

RESULTS AND DISCUSSION

Effect of ATH content on the flammability of EVM/ATH/SiO_2 composites.

Cone calorimeter test

Cone calorimeter test based on the oxygen consumption principle has been widely used to evaluate the flammability characteristics of materials. Although cone calorimeter test is a small-scale test, the obtained results have been found to correlate well with those obtained from a large-scale fire test and can be used to predict the combustion behavior of materials in a real fire.[20] For instance, the heat release rate (HRR) is a very important parameter, and can be used to express the intensity of a fire.[23] A highly flame retardant system normally shows a low HRR value.

In this research work, cone calorimeter results at a flux of 35 kW/m^2 are shown in Figure 1-Figure 3 and Table II. Figures 1 and 2 shows respectively, the dynamic curves of HRR and THR versus burning time for flame retardant EVM/ATH/SiO_2 composites. It can be found that the sample EVM-1 burns very fast. Very sharp HRR and THR curves appears at the range of 55–245 s. Whereas the PHRR and THR of flame retardant EVM/ATH/SiO_2 composites decline dramatically and also show prolongation of the combustion times. Meanwhile, the THR and average heat release rate (Aver HRR) of flame retardant EVM/ATH/SiO_2 composites are reduced. All these evince that the flame retardant of EVM/ATH/SiO_2 composites are improved dramatically.

One of the primary parameters responsible for decreasing the HRR and THR of materials is the mass loss rate (MLR) during combustion. Figure 3 is the dynamic curves of mass loss versus burning time for flame retardant EVM/ATH/SiO_2 composites. The change of mass loss is often relative to the solid-state flame retardant mechanism. From Figure 3 it can be seen that the curves of flame retardant EVM/ATH/SiO_2 composites become more and

TABLE II
Cone Calorimeter Results of Flame Retardant Composites Filled with ATH at Different Loadings

Sample Code	EVM-1	EVM-2	EVM-3	EVM-4	EVM-5
TTI (s)	57	118	155	394	—
PHRR (kW/m^2)	877	319	194	131	24
Aver-HRR(kW/m^2)	289	140	99	67	15
THR(MJ/m^2)	96	78	72	55	11
FPI (m^2.s/kW)	0.065	0.370	0.799	3.008	—
AEHC(MJ/kg)	31	25	22	16	4
Residues(%)	5.1	26.8	36.4	40.8	47.3

TTI, time to ignition; PHRR, peak of heat release rate, expressing the intensity of a fire; Aver-HRR, average HRR within the front 200 s from heat radiation; FPI, fire performance index, the ratio of TTI and PHRR.

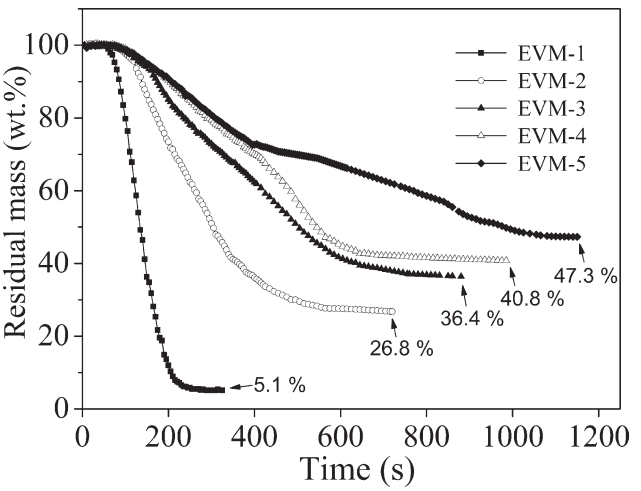

Figure 3 Residual mass versus burning time for EVM/ATH/SiO_2 composites filled with different loading of ATH

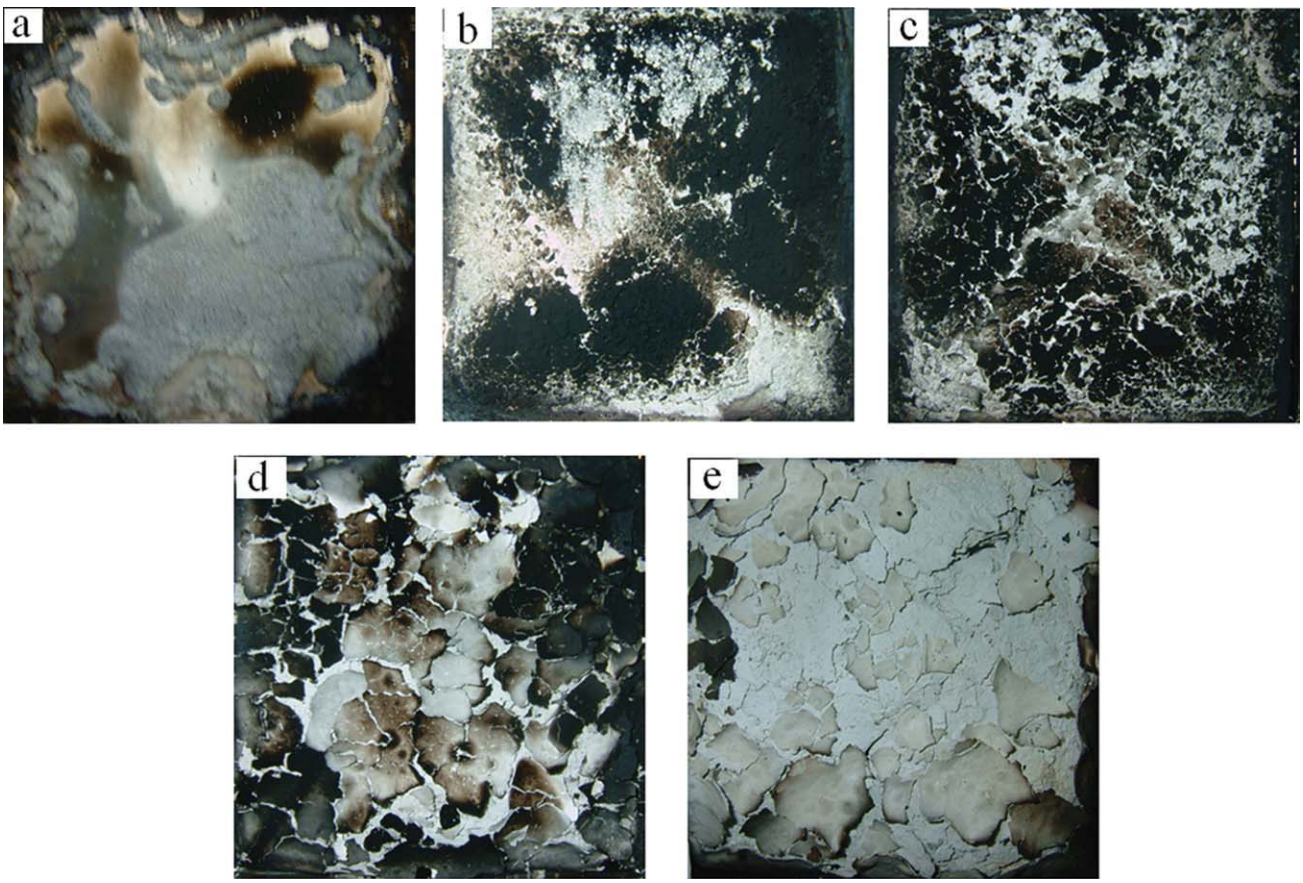

Figure 4 Original residual photographs of EVM/ATH/SiO_2 composites after fire in cone calorimeter: a) EVM-1; b) EVM-2;c) EVM-3;d) EVM-4;e) EVM-5. [Color figure can be viewed in the online issue, which is available at wileyonlinelibrary.com]

more smooth as the loading of ATH increases. The residue mass of flame retardant EVM/ATH/SiO_2 composites EVM-2, EVM-3, EVM-4, and EVM-5 are respectively, 26.8%, 36.4%, 40.8%, and 47.3%, while the combustion of the sample EVM-1 is nearly complete within 300 s and only remains 5.1% of residue, and which can be seen visually from original residue images of EVM/ATH/SiO_2 composites after fire by cone calorimeter (Fig. 4). From Figure 4 it can be found that EVM-1 without ATH [Fig. 4(a)] has been nearly burnt out and most of the aluminum foil become visual, while the others for the flame retardant EVM/ATH/SiO_2 composites remains more or less residues and incumbent nearly or completely on the aluminum foil. The sample EVM-5 [Fig. 4(e)] with a loading of 200 phr ATH presents the most and compact residue, and there are some rigid and curly slices over the surface due to the flame and heat radiation.

Figure 5 is the dynamic evolution for the sample EVM-5 during cone calorimeter experiment. From this picture it can be seen that the sample is intumescent (e_2) due to the effect of heat radiation and flame at beginning, and then charring on the surface (e_3). As the accumulation of heat, it can be found that the surface char is gradually destroyed because it cannot resist the sustaining heat radiation. Finally, only gray residue remains over the aluminum foil for EVM-5 (e_6). So it does not form bright fire and only afterglow appears for the sample EVM-5, and no typical phenomenon of polymer materials appears in the combustion, such as shrinkage, melting, etc. This just gives the reason that the PHRR and THR are so lower and the curves are so smooth for the sample EVM-5. On the other hand, it can also be found that the HRR curves of flame retardant samples EVM-2 and EVM-3 present double peaks, e.g., one peak appears at 120 s and another at 310 s from ignition for EVM-2. This indicates that the first charring appears at 120 s after radiation, and accordingly the PHRR begins to decrease. Because the char is not rigid enough to resist the continuous heat and flame, afterward it may be destroyed and the second peak of HRR appears again. This may be one of the reasons that very high loading of ATH is needed to meet necessary flame retardant level. Furthermore, from Table II it can be found that the average effective heat of combustion (AEHC) decreases gradually as the increase of ATH concentration; e.g., the AEHC of sample EVM-5 is 4

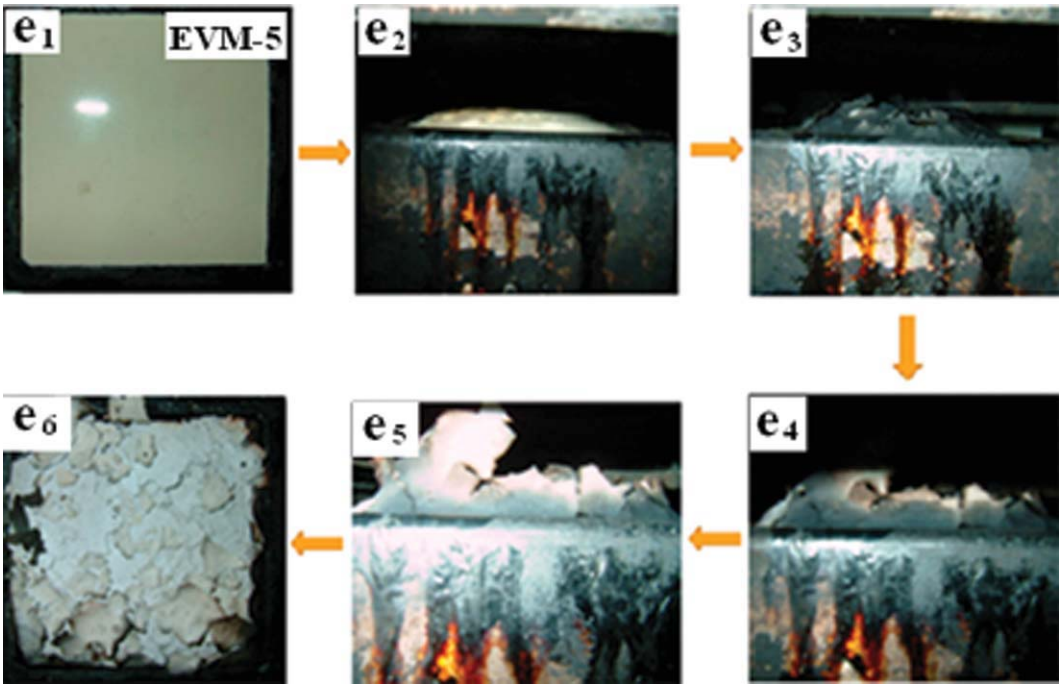

Figure 5 The dynamic evolution of afterglow (e_1-e_6) for the sample EVM-5 in cone calorimeter. [Color figure can be viewed in the online issue, which is available at wileyonlinelibrary.com]

MJ/kg, while the sample EVM-1 is 31 MJ/kg. This can show that the flame retardant mechanism of ATH mainly comes from solid phase, i.e., the release of water hydrosphere and the endothermic reaction in combustion, and meanwhile there is a stiff layer forming over the surface of materials during combustion. This can be testified from the SEM image of residues for EVM/ATH/SiO_2 composites.

Figure 6 is the microstructure of residues for the samples of EVM-1 [Fig. 6(a_1,a_2)], EVM-3 [Fig. 6(b_1,b_2)] and EVM-5 [Fig. 6(c_1,c_2)] after fire in cone calorimeter. It can be found that there only few lamellar residues [Fig. 6(a_1,a_2)] are for the sample EVM-1, and it may be brought by the flocculation of SiO_2 in fire. Because the loading of SiO_2 is small and it is lower flame retardant efficiency, the improvement of flame retardant to EVM vulcanizates is quite limited. Compared with that, there are many globular materials over the aluminum foil in the range from several dozen nanometers to several microns for EVM-3 [Fig. 6(b_1,b_2)] and EVM-5 [Fig. 6(c_1,c_2)], and the accumulation is more compact for the EVM-5. The residue may be mainly the aluminum trioxide because of the water release of ATH in fire. Moreover, it can also be found that the ignition time (TTI) and fire performance index (FPI) are heightened gradually as the loading of ATH increases, i.e., the TTI increases to 118 s, 155 s, and 394 s respectively, for EVM-2, EVM-3 and EVM-4 from 57 s for EVM-1, and the FPI increases to 0.370 m^2 s/kW, 0.799 m^2 s/kW, and 3.008 m^2 s/kW respectively, for EVM-2, EVM-3 and EVM-4 from 0.065 m^2 s/kW of EVM-1. The FPI is defined as the ratio of TTI to PHRR. Because of the close relationship between FPI and the real fire condition, it is often the basis of escape time designing for firemen in real fire. The longer the TTI and the lower the PHRR, the higher the FPI and the better chance reduce the loss and casualty in real fire. As a whole, the above results indicate that the flame retardant is dramatically improved for EVM vulcanizates by the addition of ATH, and which is very important for the practical usage as HFFR cable materials.

LOI and UL-94 tests

LOI and UL-94 vertical tests are widely used to evaluate the FR properties of materials and to screen FR formulations especially in industry. LOI is defined as the minimum fraction of oxygen in an oxygen-nitrogen mixture that is just sufficient to sustain combustion of the specimen after ignition, which represents the ability to endure fire for materials. The higher the LOI values, the higher ability to resist fire, and more difficulty to be ignited for materials. It is commonly recognized that the LOI of higher than 26% for polymer materials is necessary in industry. And especially for HFFR cable materials the LOI value must be higher than 30%. UL-94 vertical test is a very strict FR test method mainly for self-extinguish materials. It can clarify the materials

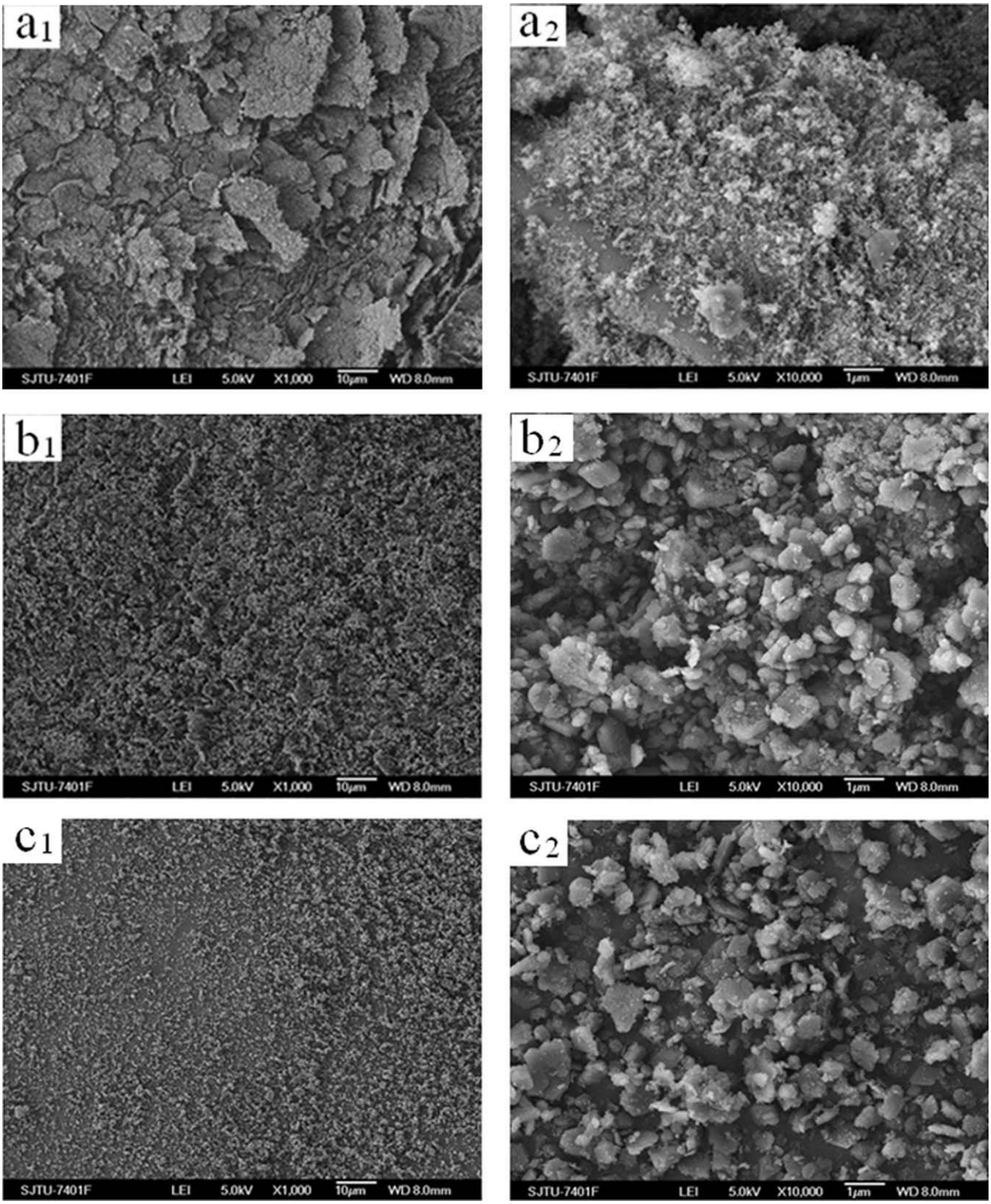

Figure 6 The microstructure of residues by FE-SEM for the samples of EVM-1 (a), EVM-3 (b) and EVM-5 (c) after combustion by cone calorimeter.

to some different grades including V-0, V-1, V-2 and no rating according to the corresponding criterion. It is usually the essential requirement for HFFR cable materials to pass V-0 of UL-94.

In this research, Table III is the LOI and UL-94 results of flame retardant EVM/ATH/SiO_2 composites. From this table, it can be found that the LOI value increases dramatically as the ATH loading

TABLE III
LOI and UL-94 Results of Flame Retardant EVM Composites Filled with ATH at Different Loadings

Sample code	LOI (%)	UL-94 vertical test		
		Rate	Ignition time (s)	Phenomenon
EVM-1	18.5	No rate	4	melt dripping heavily
EVM-2	25.0	No rate	13	melt dripping
EVM-3	34.0	V-0	24	no dripping
EVM-4	42.0	V-0	>80	no dripping
EVM-5	50.0	V-0	No ignition	afterglow

increases. The LOI increases to 25.0%, 34.0%, 42.0%, and 50.0% respectively, for the sample EVM-2, EVM-3, EVM-4, and EVM-5 from 18.5% of EVM-1. This indicates that the flame retardant of EVM/ATH/SiO_2 composites is improved gradually. Meanwhile, the UL-94 results reveal that the ignition time is prolonged and the melting antidripping is improved. Moreover, the sample EVM-5 cannot be ignited within 200 s and only present afterglow for several seconds. The samples with higher concentrations than a loading of 120 phr ATH can pass V-0 rating for EVM-3, EVM-4, and EVM-5, while the other two samples present no rating for EVM-1 and EVM-2 because of the heavy melt dripping and acute burning. All the above results indicate that the flame retardant of EVM vulcanizates have been improved evidently. Meanwhile, it is necessary that enough loading of ATH ($\geq$55 wt %) is needed to satisfy the essential flame retardant level for EVM as HFFR cable materials.

Thermal degradation behavior of EVM/ATH/SiO_2 composites

Thermal gravimetric analysis is a very common characterizing method in the field of material research. It is often used to analyze the thermal degradation behavior of FR polymer materials. Figure 7 presents the thermogravimetric (TG) and derivative TG (DTG) curves of EVM/ATH/SiO_2 composites under a flow of air. It can be found that the TG curve of ATH only present one-step process in the range of 210–290°C which is the dehydration reaction of ATH, and its corresponding DTG peak is about 260°C. On the other hand, the flame retardant EVM/ATH/SiO_2 composites show a two-step weight loss. The first step is considered to involve the dehydration reaction of ATH and the loss of acetic acid in the range of 270–380°C. The onset temperature of degradation for flame retardant EVM/ATH/SiO_2 composites with ATH is about 5–10°C lower than the sample EVM-1 due to the dehydration of ATH at lower temperature. The biggest degradation speed of flame retardant EVM/ATH/SiO_2 composites is lower than the sample EVM-1 in the first step similar as in the second step. It is testified that EVM vulcanizates have been protected to some extent just by the degradation of ATH as the sacrifice. The second step is due to the volatilization of the residual polymer at temperatures between 380 and 510°C. Finally, the residues of flame retardant EVM/ATH/SiO_2 composites gradually increases at 800°C as the loading of ATH, e.g., the residues are 28.4% and 42.8% for EVM-2 and EVM-5, respectively, while it is only 7.6% for the sample EVM-1. All these results indicate that the thermal stability of EVM vulcanizates is improved, and this is very helpful to improve its flame retardant.

The gel content and mechanical properties of EVM/ATH/SiO_2 composites

As the above depiction, it is necessary to add high loading of metal hydroxide for the HFFR polymer

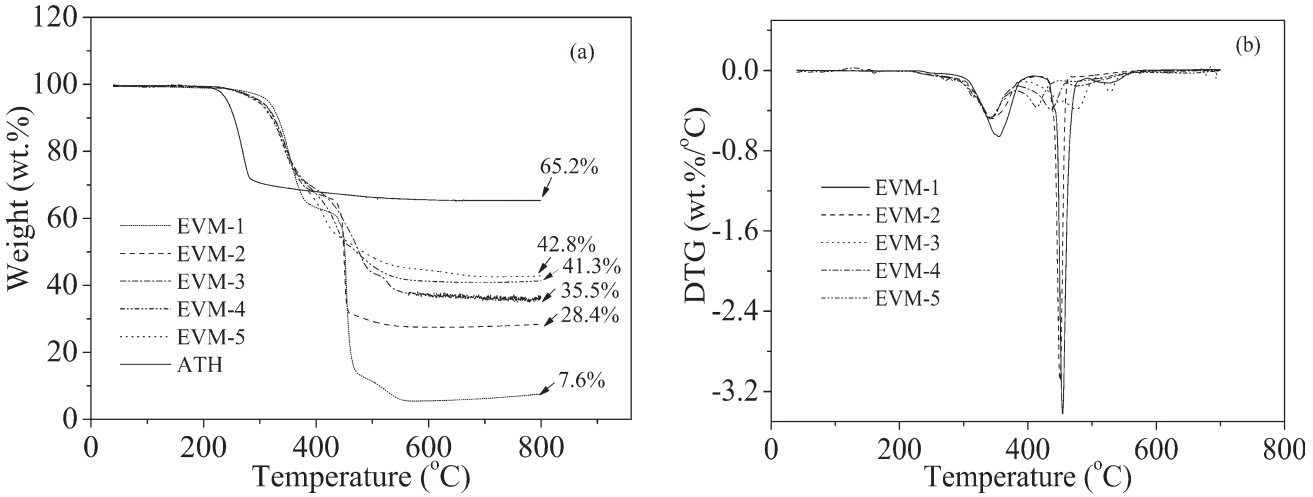

Figure 7 TG (a) and DTG (b) curves versus temperature for EVM/ATH/SiO_2 composites.

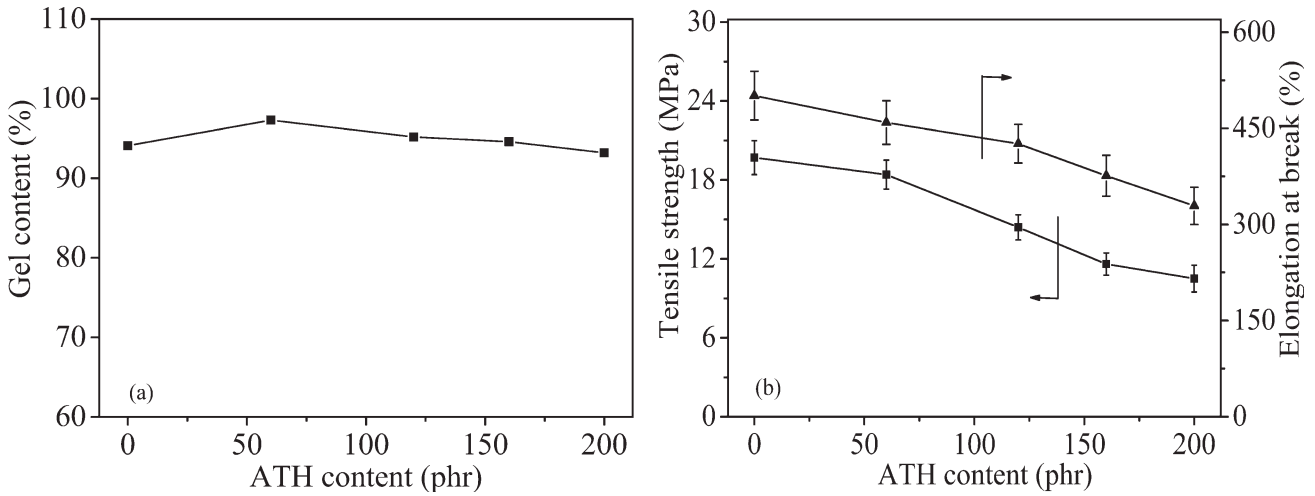

Figure 8 The gel content (a) and tensile properties (b) versus the ATH loading for EVM/ATH/SiO_2 composites.

materials to be used practically. And there is a problem that too high loading of inorganic fillers can deteriorate the mechanical property, dielectric breakdown strength, etc. So this must be considered in practical industry. Gel content measurement is usually carried out for determining the crosslinking degree of crosslinked samples: the higher gel content is due to the greater crosslinking reaction. Moreover, the mechanical properties are often influenced by gel contents for crosslinked polymer materials. Figure 8 shows the changes of the gel contents (a) and the tensile properties (b) versus the loading of ATH for flame retardant EVM/ATH/SiO_2 composites. From the above picture of Figure 8(a), it can be found that the gel contents of the samples EVM-2, EVM-3, EVM-4 and EVM-5 change to 97.3%, 95.2%, 94.6%, and 93.2%, respectively, from 94.1% of EVM-1. This indicates that the high crosslinking degree can be obtained by DCP for HFFR materials even at high loading of fillers. On the one hand, the tensile strength and elongation at break are good for the sample EVM-1 by the addition of intensifier SiO_2. The excellent compatibility can be obtained between EVM matrix and SiO_2 fillers modified with coupling agent. The modified filler SiO_2 can increase the physical crosslinking as the rigid gel and improve the mechanical properties of EVM vulcanizates. On the other hand, it can be found that the tensile strength and elongation at break decrease gradually as the loading of ATH increases. It can be concluded that the reason of deterioration must be the poor dispersion and too much congeries of ATH at high loadings. After all, the EVM vulcanizates still present good flexible properties, e.g., the elongation is higher than 300% and the strength is bigger than 10 MPa for the sample EVM-5. This is very important for its practical usage as HFFR cable materials in industry.

The dielectric properties of EVM/ATH/SiO_2 composites

The resistivity and breakdown strength are very important parameters for materials to be used as cable insulation and sheath. Figure 9 are the results of dc resistivity and ac breakdown strength for HFFR EVM/ATH/SiO_2 composites. It can be seen that the dc resistivity increases slightly for the samples at a relative low loading of ATH ($\leq$60 phr). Afterwards, the dc resistivity and ac breakdown strength decrease slightly as the loading of ATH. This may be induced by the poor dispersion and too much congeries at high loadings of ATH. On the other hand, it can be seen that the sample EVM-5 still retain the relative high ac breakdown strength and dc resistivity. After all, it presents the ac breakdown strength of higher than 21 kV/mm and dc resistivity of 1.0×10^{13} Ω.mm the same order of magnitude as the sample of EVM-1. So it is very important for

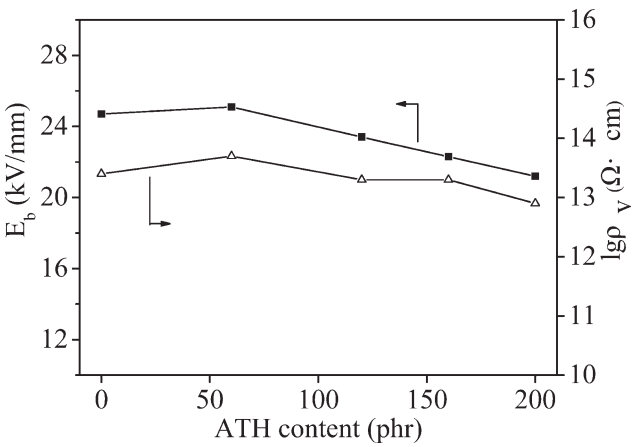

Figure 9 The dielectric breakdown strength (E_b) and dc resistivity (ρ_v) versus the loading of ATH for composites

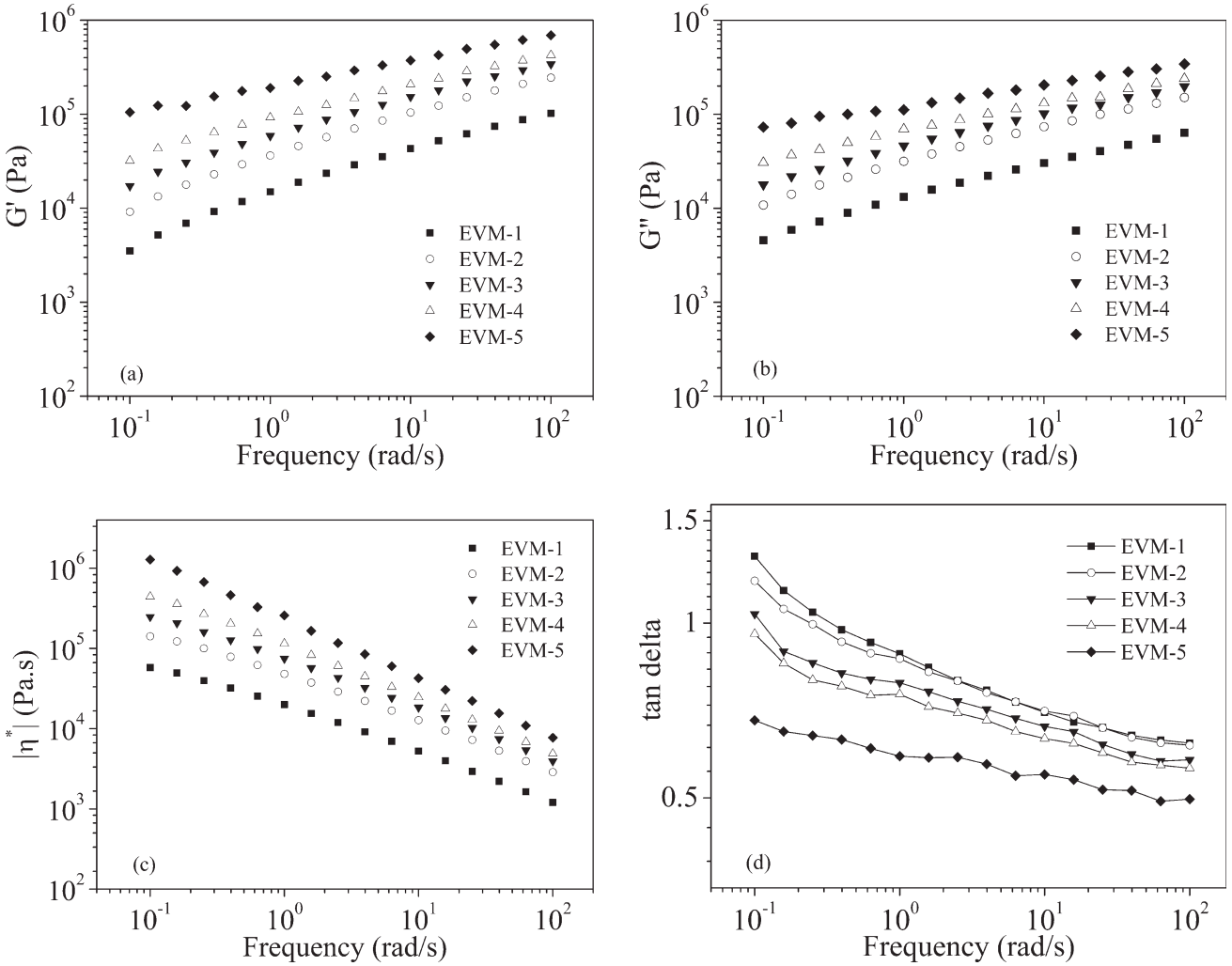

Figure 10 The storage modulus G' (a), loss modulus G'' (b), complex viscosity η* (c) and tan delta (d) versus frequency for EVM/ATH/SiO$_2$ composites.

HFFR EVM/ATH/SiO$_2$ composites with high loadings to be used practically as cable materials in industry.

The rheological properties of EVM/ATH/SiO$_2$ composites

The rheological characteristics of polymer composites are very significant because of its close relation to the practical processing and scientific importance as a probe for dynamics and microstructures of the composites,[27–30] and thus the HFFR EVM/ATH/SiO$_2$ composites have been further investigated from the viewpoint of their dynamic rheological properties. Figure 10 is the experimental results for the various rheological parameters including storage modulus, loss modulus, complex viscosity and tan delta of EVM/ATH/SiO$_2$ composites. It can be clearly seen in Figure 10(c) that the viscosity increases gradually as the loading of ATH increases. All the samples show the strong shear thinning effect (the complex viscosity almost or completely decreases linearly with the increasing frequency), and the reduction gradient of complex viscosity is more and more evident as the contents of ATH increases. Figure 10(a) shows that the storage modulus G′ of the composites increases monotonously at all the measurement frequencies as the concentration of ATH filler increases, and such an increase in the storage modulus is consistent with an increase in complex viscosity with the content of ATH increasing. Especially the increases in the complex viscosity, storage and loss modulus are observed obviously at low frequencies. A transition of the curve slopes can be found in Figure 10(a,b); the higher the loading of ATH fillers in composites, the further the curves of storage modulus G' versus frequency or loss modulus G'' versus frequency are flattened, respectively; and a plateau

would appear at a lower frequencies than 0.1 rad/s for EVM-5. The low-frequency plateau is indicative of a "pseudosolid-like" behavior,[28] and the "pseudo-solid-like" behavior may be derived from the polymer-fillers agglomerates network structure formed in the HFFR EVM/ATH/SiO_2 composites with high loadings. The percolation threshold can appear in the EVM/ATH/SiO2 composites with high loadings, and this plateau phenomenon originates from the more compactly interacted structure of ATH. Tan delta as the ratio of storage modulus with loss modulus is sensitive to the structural changes of the materials and can be widely used to study the damping characteristics of composites. It can be clearly found in Figure 10(d) that tan delta decreases monotonously in the total frequency range for all the HFFR EVM/ATH/SiO_2 composites while the plot of tan delta versus frequency presents a trend of gradually flattening for the sample EVM-5 at low frequency range.

CONCLUSIONS

The HFFR EVM/ATH/SiO_2 composites have been prepared by the melting compounding method, and the chemical way was used to the crosslinking of composites by DCP. Through the tests of combustion behavior and thermal stability, it can be found that the flame retardant is improved and the fire jeopardizing is dramatically reduced. All this can be the scientific data of fire prevention in future. The ultimate tensile strength, elongation at break, dc resistivity, and ac breakdown strength have been investigated for the HFFR EVM/ATH/SiO_2 composites; it has been found that even at very high loadings of filler, the composites still keep the mechanical and electrical properties good enough to be used practically as cable. The rheological characteristics show that the storage and loss modulus of the composites increase monotonously at all the measurement frequencies as the concentration of ATH increases, while the complex viscosity and tan delta present reverse trend. At low frequencies, the curves of storage and loss modulus versus frequency tend to approach a plateau for the sample EVM-5, representing a "pseudosolid-like" behavior derived from the polymer-filler agglomerates network structure.

References

1. Cardenas, M. A.; Garcia-Lopez, D.; Gobernado-Mitre, I.; Merino, J. C.; Pastor, J. M.; Martinez, J. D.; Barbeta, J.; Calveras, D. Polym Degrad Stab 2008, 93, 2032.
2. Horrocks, A. R.; Nazaré, S.; Kandola, B. K. Fire Safety J 2004, 39, 259.
3. Wu, C. S.; Liu, Y. L.; Chiu, Y. S. Polymer 2002, 43, 1773.
4. Hirschler, M. M.; Piansay, T. Fire Mater 2007, 31, 373.
5. Hull, T. R.; Quinn, R. E.; Areri, I. G.; Purser, D. A. Polym Degrad Stab 2002, 77, 235.
6. Wang, Z. Z.; Qu, B. J.; Fan, W. C.; Huang, P. J Appl Polym Sci 2002, 81, 206.
7. Bodzay, B.; Marosfoi, B. B.; Igrics, T.; Bocz, K.; Marosi, G. J Anal Appl Pyrol 2009, 85, 313.
8. Beyer, G. J Fire Sci 2005, 23, 75.
9. Digges, K. H.; Gann, R. G.; Grayson, S. J.; Hirschler, M. M.; Lyon, R. E.; Purser, D. A.; Quintiere, J. G.; Stephenson, R. R.; Tewarson, A. Fire Mater 2008, 32, 249.
10. Fu, M. Z.; Qu, B. J Polym Degrad Stab 2004, 85, 633.
11. Coran, A. Y. J Appl Polym Sci 2003, 87, 24.
12. Sirisinha, K.; Kamphunthong, W. Polym Test 2009, 28, 636.
13. Wang, Q.; Xiang, L.; Zhang, Y. C.; Jin, Y. J Mater Sci 2008, 43, 2387.
14. Lv, J. P.; Liu, W. H. J Appl Polym Sci 2007, 105, 333.
15. Wei, P.; Han, Z. D.; Xu, X. N.; Li, Z. X. J Fire Sci 2006, 24, 487.
16. Jiao, C. M.; Chen, X. L. J Appl Polym Sci 2010, 116, 1889.
17. Wang, S. F.; Zhang, Y.; Zhang, Y. X.; Zhang, C. M.; Li, E. J. J Appl Polym Sci 2004, 91, 1571.
18. Lu, H. D.; Hu, Y.; Yang, L.; Wang, Z. Z.; Chen, Z. Y.; Fan, W. C. J Mater Sci 2005, 40, 43.
19. Khonakdar, H. A.; Jafari, S. H.; Haghighi-Asl, A.; Wagenknecht, U.; Häussler, L.; Reuter, U. J Appl Polym Sci 2007, 103, 3261.
20. Bhattacharya, A. Prog Polym Sci 2003, 25, 371.
21. Du, A. H.; Peng, Z. L.; Zhang, Y.; Zhang, Y. X. Polym Test 2002, 21, 889.
22. Li, Z. Z.; Qu, B. J Radiat Phys Chem 2004, 69, 137.
23. Du, A. H.; Peng, Z. L.; Zhang, Y.; Zhang, Y. X. J Appl Polym Sci 2003, 89, 2192.
24. Marney, D. C. O.; Russell, L. J.; Mann, R. Fire Mater 2008, 32, 357.
25. Nazaré, S.; Kandola, B. K.; Horrocks, A. R. Polym Adv Tech 2006, 17, 294.
26. Huang, X. Y.; Jiang, P. K.; Kim, C.; Liu, F.; Yin, Y. Euro Polym J 2009, 45, 377.
27. McNally, T.; Potschke, P.; Halley, P.; Murphy, M.; Martin, D.; Brennan, G. P.; Bein, D.; Lemoine, P.; Quinn, J. P. Polymer 2005, 46, 8222.
28. Pötschke, P.; Abdel-Goad, M.; Alig, I.; Dudkin, S.; Lellinger, D. Polymer 2004, 45, 8863.
29. Moniruzzaman, M.; Winey, K. I. Macromolecules 2006, 39, 5194.
30. Kota, A. K.; Cipriano, B. H.; Duesterberg, M. K.; Gershon, A. L.; Powell, D.; Raghavan, S. R.; Bruck, H. A. Macromolecules 2007, 40, 7400.